THE JOURNAL OF PHYSICAL CHEMISTRY B

pubs.acs.org/JPCB Article

Extreme Catalytic Power of Ketosteroid Isomerase Related to the Reversal of Proton Dislocations in Hydrogen-Bond Network

Paweł Kędzierski,* Maria Zaczkowska, and W. Andrzej Sokalski*

Cite This: *J. Phys. Chem. B* 2020, 124, 3661−3666 Read Online

ACCESS | Metrics & More | Article Recommendations | Supporting Information

ABSTRACT: Dynamic electrostatic catalytic field (DECF) vectors derived from transition state and reactant wavefunctions for the two-step reaction occurring within ketosteroid isomerase (KSI) have been calculated using MP2/aug-cc-pVTZ and lower theory levels to determine the magnitude of the catalytic effect and the optimal directions of proton transfers in the KSI hydrogen-bond network. The most surprising and meaningful finding is that the KSI catalytic activity is enhanced by proton dislocations proceeding in opposite directions for each of the two consecutive reaction steps in the same hydrogen network. Such a mechanism allows an ultrafast switching of the catalytic proton wire environment, possibly related to the exceptionally high KSI catalytic power.

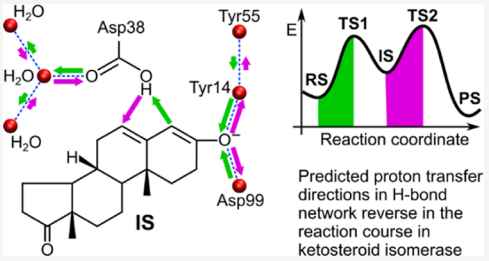

INTRODUCTION

Proton transfer between hydrogen-bonded biomolecules is one of the most important phenomena in biology. In particular, recent studies indicate that the catalytic activities of numerous enzymes are closely related to the proton transfer in hydrogen-bond chains extending from the active site.[1−8] For example, recent experimental evidence indicates that change in the proton position in the second shell residues forming the hydrogen-bond chain enhances the rate of catalysis in aspartate aminotransferase.[1] Due to the large size of the involved molecular systems and usually insufficient information regarding the positions of hydrogen atoms, the corresponding molecular mechanisms could not be easily explored by conventional experimental or theoretical methods. Therefore, for the purpose of this work, we use a more cautious term "proton dislocation", which is more adequate for short and strong hydrogen bonds, where the degree of partial proton transfer is usually not known precisely.

The aim of this contribution is to apply for the first time a method allowing the identification of the magnitude of dynamic catalytic effects and the preferred proton dislocation directions in hydrogen-bond chains extending from reactants and leading to a reduction in the activation barrier. For this purpose, we decided to test a new application of dynamic electrostatic catalytic fields (called thereafter as DECFs), defined here as the difference of the transition-state and substrate electric fields at the midpoint of every hydrogen bond, which constitutes catalytic environment. Although the theoretical concept of DECF had been originally introduced earlier,[9,10] it has not been practically applied to any enzyme reaction yet. This was due to considerable difference between the typical enzyme reaction timescale and much longer time required to dislocate active site residues or their side chains containing heavy atoms. However, this limitation disappears in the case of ketosteroid isomerase (KSI), where rapidly oscillating very light protons located in a relatively rigid hydrogen-bond network surrounding an active site have a chance to be coupled with the enzyme reaction coordinate. Due to the existing extensive experimental and theoretical data indicating an important role of the HB network,[11−13] KSI has been selected to test the DECF approach for the first time for an enzyme system. Whenever a strong DECF is detected, it could be regarded as the driving force for catalytic proton dislocation, possibly propagating in the neighboring HBs due to the domino effect. This way, our approach extends and supplements previous attempts of mapping proton wires in proteins.[2] However, catalytic fields are derived using a bottom-up approach, where the analysis of the charge redistribution from the reactants to the transition state yields properties of an optimal catalytic environment in a compact form,[9,10,14−18] constituting an inverse solution to the optimal catalyst problem. The only input data required to predict favorable proton-transfer directions for different reaction stages are the reaction pathway stationary points structures and the positions of electronegative atoms of the molecular environment only, which could serve as hydrogen bond proton donors or acceptors. No information about the usually doubtful positions of the hydrogen atom is necessary.

Received: February 20, 2020
Revised: April 15, 2020
Published: April 15, 2020

https://dx.doi.org/10.1021/acs.jpcb.0c01489
J. Phys. Chem. B 2020, 124, 3661−3666

METHODS

The catalytic activity could be expressed in terms of perturbation theory[8,14] as the difference of the transition state TS and substrate RS interaction energies ΔE in a catalytic environment C, constituting differential transition state stabilization energy E_{DTSS} approximating activation barrier lowering

$$E_{DTSS} = \Delta E(TS\cdots C) - \Delta E(RS\cdots C) \quad (1)$$

A detailed analysis of the electrostatic, exchange, delocalization (induction), and correlation (dispersion) E_{DTSS} constituents for chorismate mutase,[10] cAMP-dependent protein kinase,[15] ribonuclease,[16] several KSI mutants,[17] and Si → Al substitutions in zeolites[18] indicated the dominant role of the electrostatic term E_{EL}, which yields the results significantly correlated with higher theoretical (RHF, MP2) levels

$$E_{DTSS} \approx \Delta E_{EL}(TS\cdots C) - \Delta E_{EL}(RS\cdots C) \approx \sum q_i(V_i^{TS} - V_i^{RS}) \quad (2)$$

E_{DTSS} can be further approximated (1) by the sum of the products of catalyst atomic charges q_i and the difference in the molecular electrostatic potentials of the transition state V_i^{TS} and substrate V_i^{RS}. This difference defines the static catalytic field $\Delta_S(i)$, which represents the activation energy lowering resulting from the presence of a unit point charge +1 at any point "i"

$$\Delta_S(i) = V_i^{TS} - V_i^{RS} \quad (3)$$

The highest catalytic activity is achieved when charges representing a static molecular environment coincide with extremal $-\Delta_S$ values. Due to the additive nature of electrostatic interactions, $-\Delta_S$ represents the solution of the optimal catalyst problem, allowing an inverse design of the new catalysts and the rapid activity estimates of mutated enzymes.[17,19] This constitutes a bottom-up approach of catalyst design based on the knowledge of reactant charge redistribution during activation at a given reaction step.[19] It is fundamentally different from the conventional top-down methods requiring considering entire protein and numerous assumptions related to quantum mechanical/molecular mechanical (QM/MM) boundaries, selection of protonation states, and arbitrary empirical force fields.

As the rigid structure of the catalyst C is assumed to be derived from the static catalytic fields Δ_S, the coupling of reaction coordinates with much slower protein motions cannot be then considered. However, it is well known that rate-promoting residue vibrations could be detected in some enzymes[20] and certainly rapid oscillations of protons in hydrogen bonds could couple directly with reaction coordinates. Let us define, for a given hydrogen bond between atoms X and Y, the quantity $\overrightarrow{\Delta_D}$ as a negative gradient vector field Δ_S calculated along the line connecting X and Y at its middle point (eq 4). Such a one-dimensional dynamic electrostatic catalytic field (DECF) would therefore indicate the direction of the favorable unit probe charge movement with respect to reactants, resulting in a further decrease of the activation barrier (this idea has been illustrated in Figure 1 in ref 9 and expressed in eqs 4 and 5 in ref 9 and eq 16 in ref10). In general, the three-dimensional −grad Δ_S could be oriented in any direction and the DECF magnitude is the fraction of its length. In other words, $\overrightarrow{\Delta_D}$ vector indicates the optimal direction of proton movement in a linear hydrogen bond, leading to an increase in catalytic activity. In case of the same coordinates of atoms X and Y in both RS and TS structures, Δ_D can be rigorously calculated as the difference of the electric field vectors $\overrightarrow{E^{TS}}$ and $\overrightarrow{E^{RS}}$ located in the middle of hydrogen bond X−H···Y, projected on the X···Y bond axis described by $\vec{r}_X$ and $\vec{r}_Y$ position vectors

$$\overrightarrow{\Delta_D} = \frac{\left[\left(\overrightarrow{E^{TS}} - \overrightarrow{E^{RS}}\right)\cdot\left(\vec{r}_Y - \vec{r}_X\right)\right]}{\left|\vec{r}_Y - \vec{r}_X\right|}\cdot\frac{\vec{r}_Y - \vec{r}_X}{\left|\vec{r}_Y - \vec{r}_X\right|} \quad (4)$$

where the dot denotes a scalar product. In the following text, $\overrightarrow{\Delta_D}$ is the vector quantity of the dynamic catalytic field and Δ_D, as the signed scalar quantity, is the magnitude of $\overrightarrow{\Delta_D}$ with a positive sign if the vector is facing from X to Y and negative otherwise (i.e., the first factor of the product in eq 4). Vectors $\vec{r}_X$ and $\vec{r}_Y$ indicate the positions of X and Y atoms forming the X−H···Y hydrogen bond. Electric field vectors $\overrightarrow{E^{TS}}$ and $\overrightarrow{E^{RS}}$ are calculated at the midpoint of the hydrogen bond and then projected on the X−H···Y axis.

Equation 4 can be directly applied when the coordinates $\vec{r}_X$ and $\vec{r}_Y$ are the same in TS and RS structures, i.e., when the proton movement is the only catalytic effect. In practice, to make $\overrightarrow{\Delta_D}$ independent of the orientation of the TS and RS coordinates and to allow the application of the method to an ensemble of microstates of the catalytic complex, it can be calculated as the difference of the electric field vector projections on the X···Y axes, calculated independently for TS and RS geometries

$$\overrightarrow{\Delta_D} = \left\{\frac{\left[\overrightarrow{E^{TS}}\cdot\left(\overrightarrow{r_Y^{TS}} - \overrightarrow{r_X^{TS}}\right)\right]}{\left|\overrightarrow{r_Y^{TS}} - \overrightarrow{r_X^{TS}}\right|} - \frac{\left[\overrightarrow{E^{RS}}\cdot\left(\overrightarrow{r_Y^{RS}} - \overrightarrow{r_X^{RS}}\right)\right]}{\left|\overrightarrow{r_Y^{RS}} - \overrightarrow{r_X^{RS}}\right|}\right\}\cdot\frac{\overrightarrow{r_Y^{RS}} - \overrightarrow{r_X^{RS}}}{\left|\overrightarrow{r_Y^{RS}} - \overrightarrow{r_X^{RS}}\right|} \quad (5)$$

It is worth noticing that the change in X and Y coordinates may be an artifact of the computations; even when the proton dislocation is the only catalytic effect, the orientation and position of X and Y atom pair may change due to the independent optimization of each stationary structure.

Scalar values of Δ_S and $\overrightarrow{\Delta_D}$ vectors represent in compact form the electrostatic effects of outside reactants due to their charge redistribution on the reaction pathway from substrates to transition state.

Calculations include the following steps:

(a) The transition state and substrate stationary reaction structures are obtained using the standard QM/MM or ONIOM technique.[21] The QM part should include any active site residue forming covalent bonds with the reactants in the reaction course (ASP38 in KSI case). In

https://dx.doi.org/10.1021/acs.jpcb.0c01489
J. Phys. Chem. B 2020, 124, 3661−3666

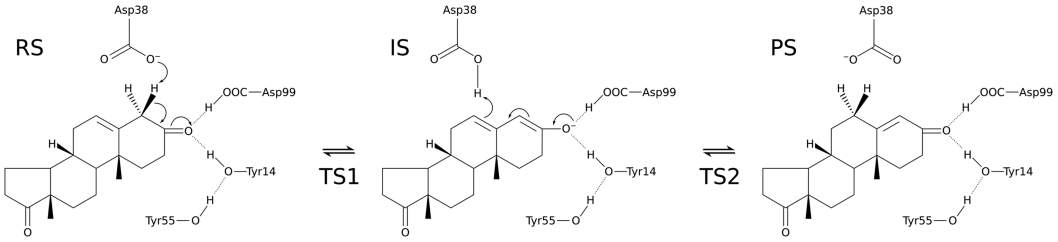

Figure 1. Mechanism of isomerization of 5-androstene-3,7-dione (RS) to 4-androstene-3,7-dione (PS) catalyzed by ketosteroid isomerase. QM part adapted from refs 17 and 21 included two first rings of the steroid and the side chain of Asp38 residue, which is involved in reactant hydrogen transfer from C4 to C6 position. This scheme constitutes a modified version of Figure 1 from our previous work (ref 17 https://pubs.acs.org/doi/10.1021/acs.jctc.6b01131) and further permissions related to the material excerpted should be directed to the ACS.

Table 1. Components of Dynamic Electrostatic Catalytic Field Δ_D Values in [au] along Hydrogen Bonds in Branched HB Chains Involving TYR14, TYR55, ASP38 Residues, and Water W1, W2, W3 Molecules for RS-TS1 and IS-TS2 Reaction Steps in Ketosteroid Isomerase Enzyme[a]

	$\Delta_D/\sum\Delta_D$ [%]		Δ_D [$\cdot 10^{-3}$ au]		cumulated $\sum\Delta_D$ [$\cdot 10^{-3}$ au]	
hydrogen bond	RS-TS1	IS-TS2	RS-TS1	IS-TS2	RS-TS1	IS-TS2
(TYR14)O···H→···O3(AND)	36.1	29.4	10.1	−8.52	27.9	−29.0
(ASP99)O···H→···O3(AND)	21.6	26.0	6.03	−7.53		
(TYR55)O···H→···O(TYR14)	10.1	9.5	2.81	−2.78		
(ASP38)O···H→···O(W1)	14.5	19.3	4.00	−5.62		
(W1)O···H→···O(W2)	9.6	8.0	2.70	−2.31		
(W1)O···H→···O(W3)	8.3	7.8	2.31	−2.27		

[a]AND stands for substrate molecule (5-androstene-3,7-dione). All results have been obtained at MP2/aug-cc-pVTZ theory level.

this work, stationary points obtained in the B3LYP/6-31+G*/CHARMM27 QM/MM approach[17,22,23] have been used.

(b) Coordinates of the entire examined protein including reaction pathway stationary points in PDB format are used as an input by the locally implemented Python script to locate all electronegative atoms located within the assumed distance from reactants (12 Å from O3 in this work) capable to form hydrogen-bonded linear and branched chains separated by a specified distance range (D = 0−3.1 Å in this work). In the case of a multistep reaction, like in KSI, it is recommended to use stationary point coordinates obtained in the same reaction coordinate scan obtained for a given reaction step and use MM minimized enzyme structure with a substrate of every step.

(c) For every hydrogen bond included in the HB chains determined earlier, expectation values of electric field vectors $\overrightarrow{E^{TS}}$ and $\overrightarrow{E^{RS}}$ are calculated at every HB midpoint, directly from the corresponding wavefunctions of reaction stationary points. Any standard quantum chemical program, like Gaussian[24] or GAMESS,[25] could be used for this purpose.

(d) The electric field vectors $\overrightarrow{E^{TS}}$ and $\overrightarrow{E^{RS}}$ are individually projected on each HB axis and then subtracted to obtain the DECF vector $\overrightarrow{\Delta_D}$ and its one-dimensional projection on the bond Δ_D, according to eq 5.

(e) A list of all hydrogen bonds forming linear or branched chains and characterized by the same Δ_D sign and DECF value above assumed threshold (0.001 au in this work) is calculated.

To visualize the results in the form of $\overrightarrow{\Delta_D}$ vectors, the program VMD (visual molecular dynamics)[26] was used.

RESULTS AND DISCUSSION

To validate our approach, we selected ketosteroid isomerase enzyme, in which proton transfer between TYR14, TYR55, and ASP99 plays a crucial role in their exceptionally high catalytic activity and has been extensively studied experimentally and theoretically.[11−13,22,23,27,28] Isomerization of 5-androstene-3,7-dione (RS) to 4-androstene-3,7-dione (PS) shown in Figure 1 proceeds in two steps via the first transition state TS1, the intermediate complex IS, and the second transition state TS2.[17,22,23] In this case, we could examine the possible catalytic role of various KSI HB chains for each reaction step, i.e., RS-TS1 and IS-TS2 separately. All stationary points have been obtained within the B3LYP/6-31+G*/CHARMM27 QM/MM setup.[17,22,23] In an analogy to our previous study related to KSI mutants,[17] the QM part included, besides reactants, the side chain of ASP38 residue directly involved in the isomerization reaction. Using MP2/aug-cc-pVTZ results presented in Table 1 as the reference, the maximum error of DECF values estimated at MP2/aug-cc-pVDZ theory level does not exceed 0.001 au, whereas same qualitative results could be still obtained from RHF/aug-cc-pVTZ or RHF/aug-cc-pVDZ (0.0015 au max error), RHF/6-311G** (0.0035 au max error), and B3LYP/6-31+G* (0.003 au max error) with a much smaller computational effort. Complete results obtained using all of the above-mentioned theory levels are presented in Table S1 in the Supporting Information along with hydrogen bond lengths. These results could be useful in selecting appropriate theory level in the case of large size reactants requiring more computational resources.

Initially, 43 hydrogen-bonded chains (D < 3.1 Å) have been detected in KSI without considering water and 81 when water at the distance of 12 Å from O3 is included. The chains of hydrogen bonds extending from substrate and active site Asp38, including water up to 12 Å from substrate O3 oxygen,

https://dx.doi.org/10.1021/acs.jpcb.0c01489
J. Phys. Chem. B 2020, 124, 3661−3666

were selected for the calculation of $\overrightarrow{\Delta_D}$. The first reaction step RS-TS1 related to the abstraction of hydrogen from the substrate C4 atom is strongly enhanced by the unidirectional proton movement from TYR14 and ASP99 to substrate oxygen O3 and from ASP38 to water W1, with additional unidirectional proton dislocations in TYR55, water W2, and W3 forming branched HB chains (Figure 2a). The second critical

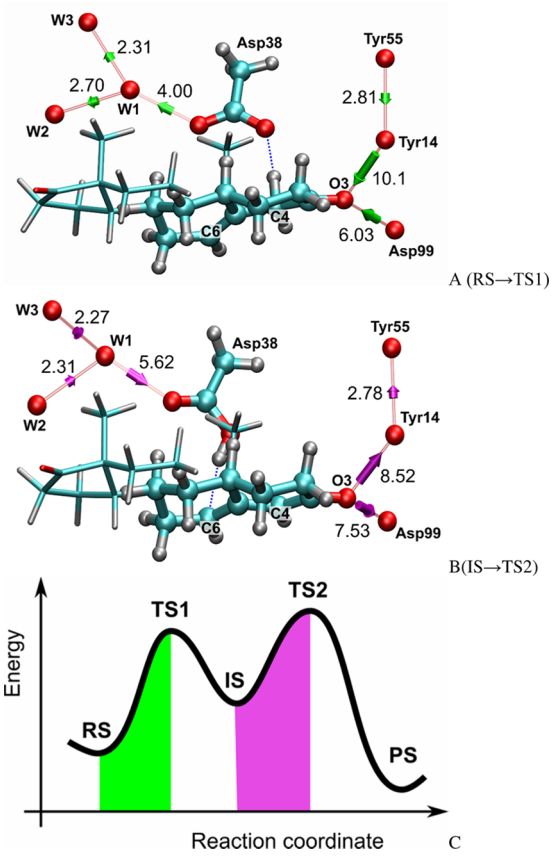

Figure 2. Directions of proton dislocations along HB chains extending from the KSI active site with relative magnitudes of catalytic effects indicated by the corresponding dynamic catalytic field vectors $\overrightarrow{\Delta_D}$ in [10^{-3} au] obtained using the MP2/aug-cc-pVTZ approach for (a) the first reaction step RS → TS1 (green arrows), (b) the second reaction step IS → TS2 (violet arrows), and (c) KSI reaction profile.[17] The part of the system included in QM calculations[17,22] presented using thicker ball-and-sticks representation.

reaction step IS-TS2 characterized by the higher activation barrier[17] (Figure 2b) is related to attaching hydrogen to the substrate carbon C6. The second reaction step IS-TS2 is strongly catalyzed by proton dislocations in the reverse directions in the same HB chains, with the dominant role of TYR14 and somewhat smaller role of water W1 and ASP38. The corresponding Δ_D and $\sum\Delta_D$ values are presented in Table 1. These results are in agreement with the recent experimental and theoretical results indicating that 98% changes of electric fields in the KSI active site originate from TYR14 and ASP99 residues.[11−13,22,23,27] Catalytic field directions obtained for the second reaction step IS → TS2 are opposite to those of the first step RS → TS1; however, the magnitudes of Δ_D and their relative $\Delta_D/\sum\Delta_D$ contributions remain very similar. This indicates that proton dislocation assisting in consecutive reaction stages RS → TS1 and IS → TS2 have to be only reversed within the same rigid hydrogen bond scaffold. Hydrogen bond lengths given in Table S1 in Supporting Information for RS, TS1, IS, and TS2 stationary points change less than 2% (0.076 A). This particular feature could be very meaningful and possibly responsible for very high KSI activity. After the completion of the first reaction step RS → TS1, minimal, possibly femtosecond, time would be required to switch the direction of proton dislocation assisting the second reaction step IS → TS2. To the best of our knowledge, such a finding has not been reported in literature yet. Similar magnitudes of Δ_D values for both reaction steps are remarkable but until more other systems are examined, we cannot definitely prove that this is not accidental. Possibly, this reflects a similar orientation of particular HB with respect to both local reaction centers at C4 and C6, as Δ_D values are more symmetric for remote HBs.

In general, computational analysis of strongly correlated multiple proton-transfer processes in hydrogen-bond chains would be extremely demanding due to its multidimensional character. On the other hand, a single proton-transfer process in the hydrogen bond characterized by the largest dynamic catalytic field Δ_D value will certainly induce additional proton dislocation in the neighboring hydrogen bonds and could constitute the driving force for a collective PT. Therefore, we consider the sum of individual DECF projections along HB axes $\sum\Delta_D$ as the quantitative measure of the catalytic activity of the entire chain and possibly connected branches. The largest relative DECF contributions $\Delta_D/\sum\Delta_D$ obtained for TYR14···AND (36.1 and 29.4%), ASP99···AND (21.6, 26.0%), and ASP38···W1 (14%, 19.3%) are in agreement with the recent path integral ab initio molecular dynamics results indicating the possibility of partial ionization of KSI ASP38, TYR14, and ASP99 residues and their dominant contribution to electric fields in the active site.[11−13,28] These conclusions are supplemented by the recent computational study of the KSI product release indicating the essential role of the ASP99 side chain.[28]

The importance of extended HB networks in KSI has been confirmed by extensive ab initio path integral molecular dynamics studies.[13] Recent independent analysis using quantum theory of atoms in molecules (QTAIM) reported a significant correlation between charge density, external electric field, and activation energy changes in KSI.[29] These results obtained by entirely different methodologies are complementary with ours reinforcing conclusions in both studies. This is in line with the well-known proton-coupled electron-transfer effects.[30]

Whereas earlier top-down computational simulations[13,28,31] focused on electric fields exerted by KSI residues on reactants, in our bottom-up approach we investigated the electric field changes, resulting from the reaction progress, acting on protons in highly polarizable HBs outside reactants. Such an inverse approach allows obtaining more detailed insight into the dynamics of the catalytic environment, which cannot be examined by the existing conventional theoretical or experimental methods.

As most of the HBs considered in this work are extremely short, possibly with a single flat minimum, the actual proton dislocation may have a partial character observed in highly polarizable HBs,[32] and in KSI in particular.[11,12]

https://dx.doi.org/10.1021/acs.jpcb.0c01489
J. Phys. Chem. B 2020, 124, 3661−3666

CONCLUSIONS

Dynamic electrostatic catalytic fields could provide new insight into the mechanisms of enzyme reactions involving extensive hydrogen-bonded networks in relatively rigid proteins with high catalytic activity, like carbonic anhydrase or green fluorescent protein.[31] The ability to reverse proton-transfer directions could also constitute an important principle in the design of theozymes aimed to catalyze multistep reactions. This approach could be also useful in scanning enzyme hydrogen-bond networks for more accurate theoretical or experimental studies related to a controversial idea of low barrier hydrogen bonds (LBHBs)[5,7] or postulated covalent nature of transition state interactions with most active enzymes, usually via hydrogen bonds.[33]

ASSOCIATED CONTENT

Supporting Information

The Supporting Information is available free of charge at https://pubs.acs.org/doi/10.1021/acs.jpcb.0c01489.

MP2/aug-cc-pVTZ, MP2/aug-cc-pVDZ, RHF/aug-cc-pVTZ, RHF/aug-cc-pVDZ, RHF/6-311G**, and B3LYP/6-31+G* and complete author lists of refs 24 and 25 (PDF)

AUTHOR INFORMATION

Corresponding Authors

Paweł Kędzierski − *Department of Chemistry, Wrocław University of Science and Technology, 50-370 Wrocław, Poland*; Email: Pawel.Kedzierski@pwr.edu.pl

W. Andrzej Sokalski − *Department of Chemistry, Wrocław University of Science and Technology, 50-370 Wrocław, Poland*; orcid.org/0000-0001-5081-8175; Email: sokalski@pwr.edu.pl

Author

Maria Zaczkowska − *Department of Chemistry, Wrocław University of Science and Technology, 50-370 Wrocław, Poland*

Complete contact information is available at: https://pubs.acs.org/10.1021/acs.jpcb.0c01489

Notes

The authors declare no competing financial interest.

ACKNOWLEDGMENTS

This research has been supported by the National Centre of Science grant NCN OPUS 2017/27/B/ST4/01327. The calculations were performed at the WCSS, ICM, and PCSS supercomputing centers. The authors are grateful to Dr. Wiktor Beker and Dr. Marc van der Kamp for providing coordinates for ketosteroid isomerase reaction stationary points. Quantum mechanical calculations were performed using Gaussian and GAMESS programs.

REFERENCES

(1) Dajnowicz, S.; Parks, J. M.; Hu, X. C.; Gesler, K.; Kovalevsky, A. Y.; Mueser, T. C. Direct evidence that an extended hydrogen-bonding network influences activation of pyridoxal 5-phosphate in aspartate aminotransferase. *J. Biol. Chem.* **2017**, *292*, 5970−5980.

(2) Shinobu, A.; Agmon, N. Proton wire dynamics in the green fluorescent protein. *J. Chem. Theory Comput.* **2017**, *13*, 353−369.

(3) Mikulski, R.; West, D.; Sippel, K. H.; Avvaru, B. S.; Aggarwal, M.; Tu, C.; McKenna, R.; Silverman, D. N. Water networks in fast proton transfer during catalysis by human carbonic anhydrase II. *Biochemistry* **2013**, *52*, 125−131.

(4) Dahms, F.; Fingerhut, B. P.; Nibbering, E. T. J.; Pines, E.; Elsaesser, T. Large-amplitude transfer motion of hydrated excess protons mapped by ultrafast 2D IR spectroscopy. *Science* **2017**, *357*, 491−495.

(5) Nichols, D. A.; Hargis, J. C.; Sanishvili, R.; Jaishankar, P.; Defrees, K.; Smith, E. W.; Wang, K. K.; Prati, F.; Renslo, A. R.; Woodcock, H. L.; Chen, Y. Ligand-induced proton transfer and low-barrier hydrogen bond revealed by X-ray crystallography. *J. Am. Chem. Soc.* **2015**, *137*, 8086−8095.

(6) Shibazaki, C.; Shimizu, R.; Kagotani, Y.; Ostermann, A.; Schrader, T. E.; Adachi, M. Direct observation of the protonation states in the mutant green fluorescent protein. *J. Phys. Chem. Lett.* **2020**, *11*, 492−496.

(7) Agback, P.; Agback, T. Direct evidence of a low barrier hydrogen bond in the catalytic triad of a Serine protease. *Sci. Rep.* **2018**, *8*, No. 10078.

(8) Grigorenko, B. L.; Knyazeva, M. A.; Nemukhin, A. N. Analysis of proton wires in the enzyme active site suggests a mechanism of c-di-GMP hydrolysis by the EAL domain phosphodiesterases. *Proteins* **2016**, *84*, 1670−1680.

(9) Sokalski, W. A. Nonempirical modeling of the static and dynamic properties of the optimum environment of for chemical reactions. *J. Mol. Struct.: THEOCHEM* **1986**, *138*, 77−87.

(10) Szefczyk, B.; Mulholland, A. J.; Ranaghan, K. E.; Sokalski, W. A. Differential transition-state stabilization in enzyme catalysis: Quantum chemical analysis of interactions in the chorismate mutase reaction and prediction of the optimal catalytic field. *J. Am. Chem. Soc.* **2004**, *126*, 16148−16159.

(11) Fried, S. D.; Bagchi, S.; Boxer, S. G. Extreme electric fields power catalysis in the active site of ketosteroid isomerase. *Science* **2014**, *346*, 1510−1514.

(12) Wang, L.; Fried, S. D.; Boxer, S. G.; Markland, T. Quantum delocalization of protons in the hydrogen-bond network of an enzyme active site. *Proc. Natl. Acad. Sci. U.S.A.* **2014**, *111*, 18454−18459.

(13) Wang, L.; Fried, S. D.; Markland, T. E. Proton network flexibility enables robustness and large electric fields in the ketosteroid isomerase active site. *J. Phys. Chem. B* **2017**, *121*, 9807−9815.

(14) Sokalski, W. A. The physical nature of catalytic activity due to molecular environment in terms of intermolecular interaction theory: Derivation of simplified models. *J. Mol. Catal.* **1985**, *30*, 395−410.

(15) Szarek, P.; Dyguda-Kazimierowicz, E.; Tachibana, A.; Sokalski, W. A. Physical nature of intermolecular interactions within cAMP-dependent protein kinase active site: Differential transition state stabilization in phosphoryl transfer reaction. *J. Phys. Chem. B* **2008**, *112*, 11819−11826.

(16) Kędzierski, P.; Sokalski, W. A.; Krauss, M. Nonempirical analysis of nature of catalytic effects in ribonuclease A active site. *J. Comp. Chem.* **2000**, *21*, 432−445.

(17) Beker, W.; van der Kamp, M. W.; Mulholland, A. J.; Sokalski, W. A. Rapid estimation of catalytic efficiency by cumulative atomic multipole moments: Application to ketosteroid isomerase mutants. *J. Chem. Theory Comput.* **2017**, *13*, 945−955.

(18) Dziekoński, P.; Sokalski, W. A.; Kassab, E.; Allavena, M. Electrostatic nature of catalytic effects resulting from Si > Al substitutions in ZSM-5 zeolite. *Chem. Phys. Lett.* **1998**, *288*, 538−544.

(19) Beker, W.; Sokalski, W. A. Bottom-up nonempirical approach reducing search space in enzyme design guided with catalytic fields. *J. Chem. Theory Comput.* **2020**, DOI: 10.1021/acs.jctc.0c00139.

(20) Wang, Z.; Chang, E. P.; Schramm, V. L. Triple isotope effects support concerted hydride and proton transfer and promoting vibrations in human heart lactate dehydrogenase. *J. Am. Chem. Soc.* **2016**, *138*, 15004−15010.

(21) Field, M. J. Simulating enzyme reactions: Challenges and perspectives. *J. Comput. Chem.* **2002**, *23*, 48−58.

(22) van der Kamp, M. W.; Chaudret, R.; Mulholland, A. J. QM/MM modelling of ketosteroid isomerase reactivity indicates that active site closure is integral to catalysis. *FEBS J.* **2013**, *280*, 3120−3131.

(23) van der Kamp, M. W.; Prentice, E. J.; Kraakman, K. L.; Connolly, M.; Mulholland, A. J.; Arcus, V. L. Dynamical origins of heat capacity changes in enzyme-catalysed reactions. *Nat. Commun.* **2018**, *9*, No. 1177.
(24) Frisch, M. J.; Trucks, G. W.; Schlegel, H. B.; Scuseria, G. E.; Robb, M. A.; Cheeseman, J. R.; Scalmani, G.; Barone, V.; Petersson, G. A.; Nakatsuji, H. et al.*Gaussian 16*, Revision C.01; Gaussian, Inc.: Wallingford CT, 2019.
(25) Schmidt, M. W.; Baldridge, K. K.; Boatz, J. A.; Elbert, S. T.; Gordon, M. S.; Jensen, J. H.; Koseki, S.; Matsunaga, N.; Nguyen, K. A.; Su, S.; et al. General atomic and molecular electronic structure system. *J. Comput. Chem.* **1993**, *14*, 1347−1363.
(26) Humphrey, W.; Dalke, A.; Schulten, K. VMD - Visual molecular dynamics. *J. Mol. Graphics* **1996**, *14*, 33−38.
(27) Chakravorty, D. K.; Hammes-Shiffer, S. Impact of mutation on proton transfer reactions in ketosteroid isomerase: Insights from molecular dynamics simulations. *J. Am. Chem. Soc* **2010**, *132*, 7549−7555.
(28) Welborn, V. V.; Head-Gordon, T. Fluctuations of electric fields in the active site of the enzyme ketosteroid isomerase. *J. Am. Chem. Soc.* **2019**, *141*, 12487−12492.
(29) Fuller, J., III; Wilson, T. R.; Eberhart, M. E.; Alexandrova, A. N. Charge density in enzyme active site as a descriptor of electrostatic preorganization. *J. Chem. Inf. Model.* **2019**, *59*, 2367−2373.
(30) Edwards, S. J.; Soudackov, A. V.; Hammes-Schiffer, S. Analysis of kinetic isotope effects for proton-coupled electron transfer reactions. *J. Phys. Chem. A* **2009**, *113*, 2117−2126.
(31) Zoi, I.; Antoniou, D.; Schwartz, S. D. Electric fields and fast protein dynamics in enzymes. *J. Phys. Chem. Lett.* **2017**, *8*, 6165−6170.
(32) Shinobu, A.; Agmon, N. Mapping proton wires in proteins: carbonic anhydrase and GFP chromophore biosynthesis. *J. Phys. Chem. A* **2009**, *113*, 7253−7266.
(33) Zhang, X. Y.; Houk, K. N. Why enzymes are proficient catalysts: Beyond the Pauling paradigm. *Acc. Chem. Res.* **2005**, *38*, 379−385.

https://dx.doi.org/10.1021/acs.jpcb.0c01489
J. Phys. Chem. B 2020, 124, 3661−3666